

# Exploring a high-level programming model for the NWP domain using ECMWF microphysics schemes

Stefano Ubbiali<sup>1</sup>, Christian Kühnlein<sup>2</sup>, Christoph Schär<sup>1</sup>, Linda Schlemmer<sup>3</sup>, Thomas C. Schulthess<sup>4,5</sup>, Michael Staneker<sup>2</sup>, and Heini Wernli<sup>1</sup>

<sup>1</sup>Institute for Atmospheric and Climate Science (IAC), ETH Zürich, Switzerland

<sup>2</sup>European Centre for Medium-Range Weather Forecasts (ECMWF), Bonn, Germany

<sup>3</sup>Deutscher Wetterdienst (DWD), Offenbach, Germany

<sup>4</sup>Institute for Theoretical Physics (ITP), ETH Zürich, Switzerland

<sup>5</sup>Swiss National Supercomputing Centre (CSCS), Lugano, Switzerland

**Abstract.** We explore the domain-specific Python library GT4Py (GridTools for Python) for implementing a representative physical parametrization scheme and the related tangent-linear & adjoint algorithms from the Integrated Forecasting System (IFS) of ECMWF. GT4Py encodes stencil operators in an abstract and hardware-agnostic fashion, thus enabling more concise, readable and maintainable scientific applications. The library achieves

5 high performance by translating the application into targeted low-level coding implementations. Here, the main goal is to study the correctness and performance-portability of the Python rewrites with GT4Py against the reference Fortran code and a number of automatically and manually ported variants created by ECMWF. The present work is part of a larger cross-institutional effort to port weather and climate models to Python with GT4Py. The focus of the current work is the IFS prognostic cloud microphysics scheme, a core physical parametrization represented by

10 a comprehensive code that takes a significant share of the total forecast model execution time. In order to verify GT4Py for Numerical Weather Prediction (NWP) systems, we put additional emphasis on the implementation and validation of the tangent-linear and adjoint model versions which are employed in data assimilation. We benchmark all prototype codes on three European supercomputers characterized by diverse GPU and CPU hardware, node designs, software stacks and compiler suites. Once the application is ported to Python with GT4Py, we find excellent

15 portability, competitive GPU performance, and robust execution in all tested scenarios including with ~~reduced~~-single precision.

## 1 Introduction

Soon after its first public release in 1957, Fortran ~~has become~~ became the language of choice for weather and climate models (Méndez et al., 2014). On the one hand, its ~~functional~~ procedural programming style and built-in support for multi-dimensional arrays has granted Fortran large popularity in the whole scientific computing community. On the other, its low-level nature guarantees fast execution of intensive mathematical operations on vector machines and conventional Central Processing Units (CPUs). In the last decades, these characteristics have permitted to run weather forecasts several times per day under tight operational schedules on High-Performance Computing (HPC) systems (Neumann et al., 2019).

In recent years, in response to the simultaneous end of Moore’s law and Dennard scaling, and due to the societal challenge to reduce energy consumption, the computer hardware landscape has been undergoing a rapid specialization to prevent unsustainable growth of the power envelope (Müller et al., 2019). As a result, most supercomputers nowadays have a heterogeneous node design, where energy-efficient accelerators such as Graphics Processing Units (GPUs) co-exist with traditional CPUs. Because Fortran has been conceived with CPU-centric machines in mind, efficient programming of hybrid HPC platforms using the core Fortran language can be challenging (Méndez et al., 2014; Lawrence et al., 2018). Indeed, the sustained performance of legacy weather and climate model codes written in Fortran has decreased over the decades (Schulthess et al., 2018), revealing the urgency for algorithmic and software adaptations to remain competitive in the medium and long term (Bauer et al., 2021).

Compiler directives (or pragmas) are an attractive solution for parallelization, both to spread a workload across multiple CPU threads, and to offload data and computations to GPU. The most famous incarnations of this programming paradigm are OpenMP (Dagum and Menon, 1998) and OpenACC (Chandrasekaran and Juckeland, 2017). Because compiler directives accommodate incremental porting and enable non-disruptive software development workflows, they are adopted by many weather and climate modeling groups, who are facing the grand challenge of accelerating large code-bases with thousands of source files and millions of lines of code, which stem from decades of scientific discoveries and software developments (Lapillonne et al., 2017, 2020; Randall et al., 2022). In order not to threaten the overall readability of the code by exposing low-level instructions, the annotation of Fortran codes with compiler directives can be automated in the pre-processor step of the compilation process using tools such as the CLAW compiler (Clement et al., 2019) or the ECMWF source-to-source translation tool Loki<sup>1</sup>. Although pragma-based programming models can support intrusive hardware-specific code transformations, additional specialized

---

<sup>1</sup>[github.com/ecmwf-ifs/loki](https://github.com/ecmwf-ifs/loki)

45 optimizations may still be required, which could finally lead to code duplication and worsen maintainability (Dahm et al., 2023). Moreover, performance and portability are much dependent on the level of support and optimization offered by the compiler stack.

On the contrary, domain-specific languages (DSLs) separate the code describing the science from the code actually executing on the target hardware, thus enabling *performance-portability*, namely application codes that achieve  
50 near-optimal performance on a variety of computer architectures (Deakin et al., 2019). Large portions of many modeling systems are being rewritten using multiple and diverse DSLs, not necessarily embedded in Fortran. For instance, the dynamical core of the weather prediction model from the COnsortium for Small-scale MOdeling (COSMO; Baldauf et al., 2011) has been rewritten in C++ using the GridTools library (Afanasyev et al., 2021) to port stencil-based operators to GPUs (Fuhrer et al., 2014, 2018). Similarly, HOMMEXX-NH (Bertagna et al., 2020)  
55 is an architecture-portable C++ implementation of the non-hydrostatic dynamical core of the Energy Exascale Earth System model (E3SM; Taylor et al., 2020) harnessing the Kokkos library to express on-node parallelism (Edwards et al., 2014). The GungHo project for a new dynamical core at the UK Met Office ([Melvin et al., 2019, 2024](#)) blends the LFRic infrastructure with the PSyclone code generator (Adams et al., 2019). Pace (Ben-Nun et al., 2022; Dahm et al., 2023) is a Python rewrite of the Finite-Volume Cubed-Sphere Dynamical Core (FV3; Harris and Lin, 2013)  
60 using GT4Py to accomplish performance-portability and productivity. Similarly, various Swiss partners including MeteoSwiss, ETH Zurich and CSCS are porting the ICOSahedral Non-hydrostatic modeling framework (ICON; Zängl et al., 2015) to GT4Py (Luz et al., 2024). In another related project (Kühnlein et al., 2023), a next-generation model for the IFS at ECMWF is developed in Python with GT4Py building on FVM (Smolarkiewicz et al., 2016; Kühnlein et al., 2019).

65 The focus of the portability efforts mentioned above is the model dynamical core - the part of the model solving numerically the fundamental nonlinear fluid-dynamics equations. In the present work, we turn the attention to physical parametrizations - which account for the representation of subgrid-scale processes - and additionally address the associated tangent-linear and adjoint algorithms. Parametrizations are being commonly ported to accelerators using OpenACC (e.g., Fuhrer et al., 2014; Yang et al., 2019; Kim et al., 2021). Wrappers around low-level legacy  
70 physics codes might then be designed to facilitate adoption within higher-level workflows (Monteiro et al., 2018; McGibbon et al., 2021). Lately, first attempts at refactoring physical parametrizations with respect to portability have been documented in the literature. For instance, Watkins et al. (2023) presented a rewrite of the MPAS-Albany Land Ice (MALI) ice-sheet model using Kokkos. Here, we present a Python implementation of the cloud microphysics

schemes CLOUDSC (Ubbiali et al., 2024c) and CLOUDSC2 (Ubbiali et al., 2024d), which are part of the physics  
 75 suite of the IFS at ECMWF<sup>2</sup>. Details on the formulation and validation of the schemes are discussed in Section 2.  
 The proposed Python implementations build upon the GT4Py toolchain, and in the remainder of the paper we use  
 the term CLOUDSC-GT4Py to refer to the GT4Py rewrite of CLOUDSC, while the GT4Py ports of the nonlinear,  
 tangent-linear and adjoint formulations of CLOUDSC2 are collectively referred to as CLOUDSC2-GT4Py. The  
 working principles of the GT4Py framework are illustrated in Section 3, where we also advocate the advantages offered  
 80 by domain-specific software approaches. Section 4 sheds some light on the infrastructure code (Ubbiali et al., 2024b),  
 and how it can enable composable and reusable model components. In Section 5, we compare the performance of  
 CLOUDSC-GT4Py and CLOUDSC2-GT4Py, as measured on three leadership-class GPU-equipped supercomputers,  
 to established implementations in Fortran and C/C++. We conclude the paper with final remarks and future  
 development paths.

## 85 2 Defining the targeted scientific applications

Several physical and chemical mechanisms occurring in the atmosphere are active on spatial scales that are significantly  
 smaller than the highest affordable model resolution. It follows that these mechanisms cannot be properly captured  
 by the resolved model dynamics, but need to be *parametrized*. Parametrizations express the bulk effect of subgrid-  
 scale phenomena on the resolved flow in terms of the grid-scale variables. The equations underneath physical  
 90 parametrizations are based on theoretical and semi-empirical arguments, and their numerical treatment commonly  
 adheres to the *single-column* abstraction, so that adjustments can only happen within individual columns, with no  
 data dependencies between columns. The atmospheric module of the IFS includes parametrizations dealing with  
 the radiative heat transfer, deep and shallow convection, clouds and stratiform precipitation, surface exchange,  
 turbulent mixing in the planetary boundary layer, subgrid-scale orographic drag, non-orographic gravity wave drag,  
 95 and methane oxidation (ECMWF, 2023).

The focus of this paper is on the cloud microphysics modules of the ECMWF: the CLOUDSC – used in operational  
 forecasting – and the CLOUDSC2 – employed in the data assimilation. The motivation is three-fold: (i) both schemes  
 are among the most computationally expensive parametrizations, with the CLOUDSC accounting for up to 10%  
 of the total execution time of the high-resolution operational forecasts at ECMWF; (ii) they are representative  
 100 of the computational patterns ubiquitous in physical parametrizations; and (iii) they already exist in the form of

---

<sup>2</sup>As we mention in Section 2, the versions of CLOUDSC and CLOUDSC2 considered in this study correspond to older release cycles  
 of the IFS than the one currently used in production.

*dwarfs*. The weather and climate “computational dwarfs”, or simply “dwarfs”, are model components shaped into stand-alone software packages to serve as archetypes of relevant computational motifs (Müller et al., 2019) and provide a convenient platform for performance optimizations and portability studies (Bauer et al., 2020). In recent years, the Performance and Portability Team of ECMWF created the CLOUDSC and CLOUDSC2 dwarfs. The  
105 original Fortran codes for both packages, corresponding respectively to the IFS Cycle 41r2 and 46r1, have been pulled out of the IFS codebase, slightly polished<sup>3</sup> and finally made available in public code repositories<sup>4</sup>. Later, the repositories have been enriched with alternative coding implementations, using different languages and programming paradigms; the most relevant implementations will be discussed in Section 5.

## 2.1 CLOUDSC: Cloud microphysics of the forecast model

110 The CLOUDSC is a single-moment cloud microphysics scheme that parametrizes stratiform clouds and their contribution to surface precipitation (ECMWF, 2023). It was implemented in the IFS Cycle 36r4 and has been operational at ECMWF since November 2010. Compared to the pre-existing scheme, it accounts for five prognostic variables (cloud fraction, cloud liquid water, cloud ice, rain and snow) and brings substantial enhancements in different aspects, including treatment of mixed-phase clouds, advection of precipitating hydrometeors (rain and snow),  
115 physical realism, and numerical stability (Nogherotto et al., 2016). For a comprehensive description of the scheme, we refer the reader to Forbes et al. (2011) and the references therein. For all the coding versions considered in this paper, including the novel Python rewrite, the calculations are validated by direct comparison of the output against serialized language-agnostic reference data provided by ECMWF.

## 2.2 CLOUDSC2: Cloud microphysics in the context of data assimilation

120 The CLOUDSC2 scheme represents a streamlined version of CLOUDSC, devised for use in the four-dimensional variational assimilation (4D-Var) at ECMWF (Courtier et al., 1994). 4D-Var merges short-term model integrations with observations over a twelve-hour assimilation window to determine the best possible representation of the current state of the atmosphere. This then provides the initial conditions for longer-term forecasts (Janisková and Lopez, 2023). The optimal synthesis between model and observational data is found by minimizing a cost function, which  
125 is evaluated using the *tangent-linear* of the *non-linear* forecasting model, while the *adjoint* model is employed to compute the gradient of the cost function (Errico, 1997; Janisková et al., 1999). For the sake of computational

---

<sup>3</sup>Compared to the original implementations run operationally at ECMWF, the CLOUDSC & CLOUDSC2 dwarf codes do not include (i) all the IFS-specific infrastructure code, (ii) the calculation of budget diagnostics, and (iii) dead code paths.

<sup>4</sup><https://github.com/ecmwf-ifs/dwarf-p-cloudsc> and <https://github.com/ecmwf-ifs/dwarf-p-cloudsc2-tl-ad>

economy, the tangent-linear and adjoint operators are derived from a simplified and regularized version of the full non-linear model. The CLOUDSC2 is one of the physical parametrizations included in the ECMWF's simplified model, together with radiation, vertical diffusion, orographic wave drag, moist convection, and non-orographic gravity wave activity (Janisková and Lopez, 2023). In the following, we provide a mathematical and algorithmic representation of the tangent-linear and adjoint versions of CLOUDSC2. For the sake of brevity, in the rest of the paper we will refer to the non-linear, tangent-linear and adjoint formulations of CLOUDSC2 using CLOUDSC2NL, CLOUDSC2TL and CLOUDSC2AD, respectively.

~~The Taylor test assessing the formal correctness of the coding implementation of the tangent-linear formulation of CLOUDSC2, denoted as CLOUDSC2TL. The three-dimensional arrays  $\mathbf{x}$  and  $\mathbf{y}$  collect the grid point values for all  $n_{in}$  input fields and  $n_{out}$  output fields of CLOUDSC2, respectively. The corresponding variations are  $\delta\mathbf{x}$  and  $\delta\mathbf{y}$ . The grid consists of  $n_{col}$  columns, each containing  $n_{lev}$  vertical levels. Note that compared to its functional counterpart  $F'[\mathbf{x}]:\delta\mathbf{x}\mapsto\delta\mathbf{y}$ ,  $\text{CLOUDSC2TL}(\mathbf{x},\delta\mathbf{x})$  returns both  $\mathbf{y}$  and  $\delta\mathbf{y}$ . The coding implementation of the non-linear CLOUDSC2 is indicated as CLOUDSC2NL.~~

```

140  total_norm ← 0 total_count ← 0 β ← |∑i=1nlev ∑k=1ncol δ $\mathbf{y}_j(i,k,l)$ | total_norm ← total_norm + |∑i=1nlev ∑k=1ncol ( $\mathbf{y}_j(i,k,l)$ 
total_count ← total_count + 1 return total_norm/total_count return 0-
    δ $\mathbf{x}$  ← 0.01 *  $\mathbf{x}(\mathbf{y},\delta\mathbf{y})$  ← CLOUDSC2TL( $\mathbf{x},\delta\mathbf{x}$ ) norms ← () jstart ← 1  $\mathbf{y}_j$  ← CLOUDSC2NL( $\mathbf{x}+10^{-j}*\delta\mathbf{x}$ )
norms ← norms ∪ (1 - TOTALNORM(ncol,nlev,nout, $\mathbf{y},\mathbf{y}_j,10^{-j}*\delta\mathbf{y}$ )) jstart ← j-
    test ← test + 10 negat ← norms(j+1) < norms(j) test ← 11 test ← test + 7 test ← test + 5 print "The
145 Taylor test passed." print "The Taylor test failed."

```

Let  $F:\mathbf{x}\mapsto\mathbf{y}$  be the functional description of CLOUDSC2, connecting the input fields  $\mathbf{x}$  with the output variables  $\mathbf{y}$ . The tangent-linear operator  $F'$  of  $F$  is derived from the Taylor series expansion

$$F(\mathbf{x}+\delta\mathbf{x})=\mathbf{y}+\delta\mathbf{y}=F(\mathbf{x})+F'[\mathbf{x}](\delta\mathbf{x})+\mathcal{O}(\|\delta\mathbf{x}\|^2), \quad (1)$$

where  $\delta\mathbf{x}$  and  $\delta\mathbf{y}$  are variations on  $\mathbf{x}$  and  $\mathbf{y}$ , and  $\|\cdot\|$  is a suitable norm. The formal correctness of the coding implementation of  $F'$  can be assessed through the Taylor test (also called the “V-shape” test), which ensures that the following condition is satisfied up to machine precision:

$$\lim_{\lambda\rightarrow 0}\frac{F(\mathbf{x}+\lambda\delta\mathbf{x})-F(\mathbf{x})}{F'[\mathbf{x}](\lambda\delta\mathbf{x})}=1 \quad \forall \mathbf{x},\delta\mathbf{x}. \quad (2)$$

The logical steps carried out in the actual implementation of the Taylor test are sketched in Algorithm A1 ([Appendix A](#)).

155 The adjoint operator  $F^*$  of  $F'$  is defined such that for the inner product  $\langle \cdot, \cdot \rangle$ :

$$\langle \delta \mathbf{x}, F^*[\mathbf{y}](\delta \mathbf{y}) \rangle = \langle \delta \mathbf{y}, F'[\mathbf{x}](\delta \mathbf{x}) \rangle \quad \forall \mathbf{x}, \delta \mathbf{x}, \mathbf{y}, \delta \mathbf{y}. \quad (3)$$

In particular, (3) must hold for  $\mathbf{y} = F(\mathbf{x})$  and  $\delta \mathbf{y} = F'[\mathbf{x}](\delta \mathbf{x})$ :

$$\langle \delta \mathbf{x}, F^*[F(\mathbf{x})](F'[\mathbf{x}](\delta \mathbf{x})) \rangle = \langle F'[\mathbf{x}](\delta \mathbf{x}), F'[\mathbf{x}](\delta \mathbf{x}) \rangle \quad \forall \mathbf{x}, \delta \mathbf{x}. \quad (4)$$

The latter condition is at the ~~hearth~~[heart](#) of the so-called symmetry test for  $F^*$  (see Algorithm A2 [in Appendix A](#)).

160 ~~The symmetry test assessing the formal correctness of the coding implementation of the adjoint formulation of CLOUDSC2, denoted as CLOUDSC2AD. The machine epsilon is indicated as  $\epsilon$ ; all other symbols have the same meaning as in Algorithm A1. Note that compared to its functional counterpart  $F^*[F(\mathbf{x})]: \delta \mathbf{y} \mapsto \delta \mathbf{x}^*$ , CLOUDSC2AD( $\mathbf{x}, \delta \mathbf{y}$ ) returns both  $\mathbf{y}$  and  $\delta \mathbf{x}^*$ .~~

```


e ← 0 ∈ ℝncol c(i) ← c(i) + ∑k=1ncol a(i, k, l) * b(i, k, l) return e
165  δx ← 0.01 * x(y, δy) ← CLOUDSC2TL(x, δx) cy ← COLUMNWISEINNERPRODUCT(ncol, nlev, nout, δy, δy)
(y, δx*) ← CLOUDSC2AD(x, δy) cx ← COLUMNWISEINNERPRODUCT(ncol, nlev, nin, δx, δx*)
success ← True c ← |cy(i)| / ε c ← |cy(i) - cx(i)| / |ε * cx(i)| success ← success & c < 103 print "The symmetry
test passed." print "The symmetry test failed."


```

### 3 A domain-specific approach to scientific software development

170 In scientific software development, it is common practice to conceive a first proof-of-concepts implementation of a numerical algorithm in a high-level programming environment like MATLAB/Octave (Lindfield and Penny, 2018), or Python. Because these languages do not require compilation and support dynamic typing, they provide a breeding ground for fast prototyping. However, the direct adoption of interpreted languages in HPC has historically been hindered by their intrinsic slowness. To squeeze more performance out of the underlying silicon, the initial proof-

175 of-concept is translated into either Fortran, C or C++. This leads to the so-called “two-language problem”, where the programming language used for the germinal prototyping is abandoned in favor of a faster language that might be more complicated to use. The lower-level code can be parallelized for shared memory platforms using OpenMP

directives, while distributed memory machines can be targeted using Message Passing Interface (MPI) libraries. The resulting code can later be migrated to GPUs, offering outstanding compute throughput and memory bandwidth especially for Single Instruction Multiple Data (SIMD) applications. GPU porting is accomplished using either OpenACC or OpenMP directives, or via a CUDA<sup>5</sup> or HIP<sup>6</sup> rewriting, amongst others. To efficiently run the model at scale on multiple GPUs, a GPU-aware MPI build should be chosen, so to possibly avoid costly memory transfers between host and device and better overlap computations and communications.

The schematic visualization in Fig. 1a highlights how the above workflow leads to multiple implementations of the same scientific application utilizing different programming models and coding styles. This unavoidably complicates software maintainability: ideally, any modification in the numerical model should be encoded in all implementations, so to preserve the coherency across the hierarchy. The maintainability problem is exacerbated as the number of lines of code, the pool of platforms to support, and the user-base increase. This situation has been known as the “software productivity gap” (Lawrence et al., 2018), and we argue that it cannot be alleviated by relying on general-purpose programming paradigms and monolithic code designs. Instead, it calls for a more synergistic collaboration between domain scientists (which here include model developers, weather forecasters, and weather and climate scientists) and computer experts. A path forward is provided by DSLs through *separation of concerns* (Fig. 1b), so that domain scientists can express the science using syntactic constructs that are aligned with the semantics of the application domain and hide any architecture-specific detail. The resulting source code is thus hardware-agnostic, more concise, easier to read, and easier to manipulate. A toolchain developed by software engineers then employs automatic code generation techniques to synthesize optimized parallel code for the target computer architecture in a transparent fashion.

### 3.1 The GT4Py framework

GT4Py<sup>7</sup> is a Python library to generate high-performance implementations of stencil<sup>8</sup> kernels as found in weather and climate applications. The library is developed and maintained by the Swiss National Supercomputing Center (CSCS), ETH Zurich, and the Swiss Federal Office of Meteorology and Climatology (MeteoSwiss), and benefits from important contributions by international partners such as the Paul Allen Institute for Artificial Intelligence (AI<sup>2</sup>). The choice of embedding the GT4Py framework in Python has been mainly dictated by the following factors: (i) Python is taught

---

<sup>5</sup><https://docs.nvidia.com/cuda/>

<sup>6</sup><https://rocm.docs.amd.com/projects/HIP/en/latest/>

<sup>7</sup><https://github.com/GridTools/gt4py>

<sup>8</sup>A *stencil* is an operator that computes array elements by accessing a fixed pattern of neighbouring items.



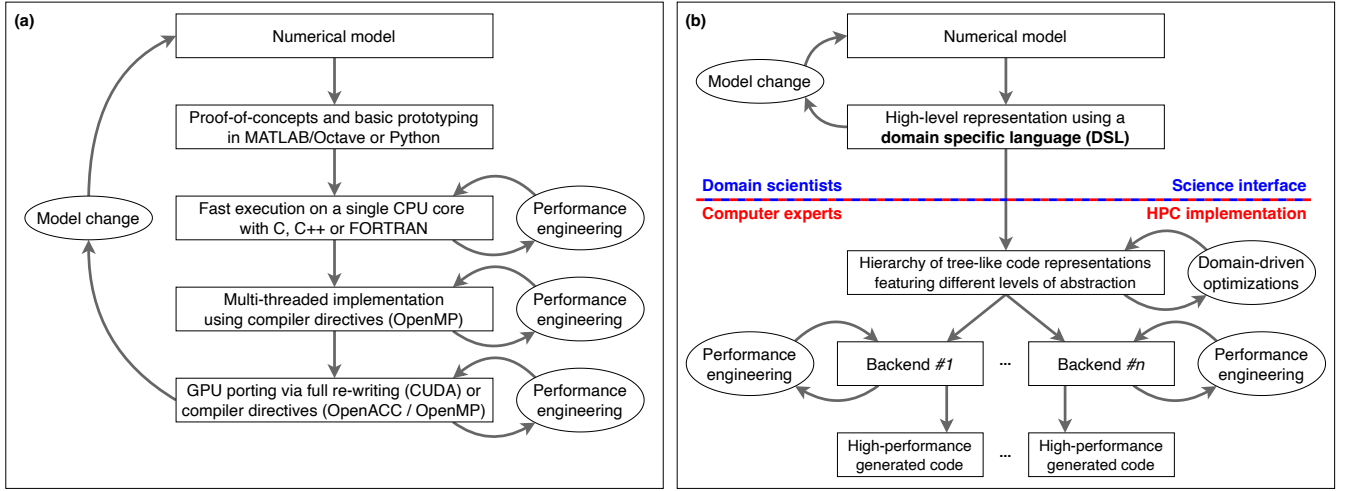


**Figure 1.** Diagrams comparing (a) a well-established workflow in scientific software development, and (b) a DSL-based approach resembling the software engineering strategy advocated in this paper. The red-and-blue dashed line in (b) mark the separation-of-concerns between the domain scientists and the computer experts.

in many academic courses due its clean, intuitive and expressive syntax, so that a significant fraction of early-career domain scientists ~~is~~are exposed to the language; (ii) it admits a powerful ecosystem of open source packages for building end-to-end applications; (iii) it is possible to seamlessly interface Python with lower-level languages with minimal overhead and virtually no memory copies; (iv) under the thrust of the Artificial Intelligence and Machine Learning community (AI/ML), the popularity and adoption of Python across the whole scientific community is constantly growing, as opposed to Fortran (Shipman and Randles, 2023). The proposed Python implementations of CLOUDSC and CLOUDSC2 are based on the first public release of GT4Py, which only supports Cartesian grids. Latest advancements to support unstructured meshes (contained in the sub-package `gt4py.next`) are not discussed in this study.

Figure 2 showcases the main steps undertaken by the GT4Py toolchain to translate the high-level definition of the horizontal Laplacian operator into optimized code, which can be directly called from within Python. The stencil definition is given as a regular Python function using the GTScript DSL. GTScript abstracts spatial for-loops away: computations are described for a single point of a three-dimensional Cartesian grid, and can be ~~differentiated~~diversified for the vertical boundaries using the `interval` context manager. Vertical loops are replaced by `computation` contexts, which define the iteration order along the vertical axis: either `PARALLEL` (meaning no vertical data dependencies between horizontal planes), `FORWARD` or `BACKWARD`. Each assignment statement within a computation block can be thought of as a loop over a horizontal plane; no horizontal data dependencies are allowed. Neighbouring points are

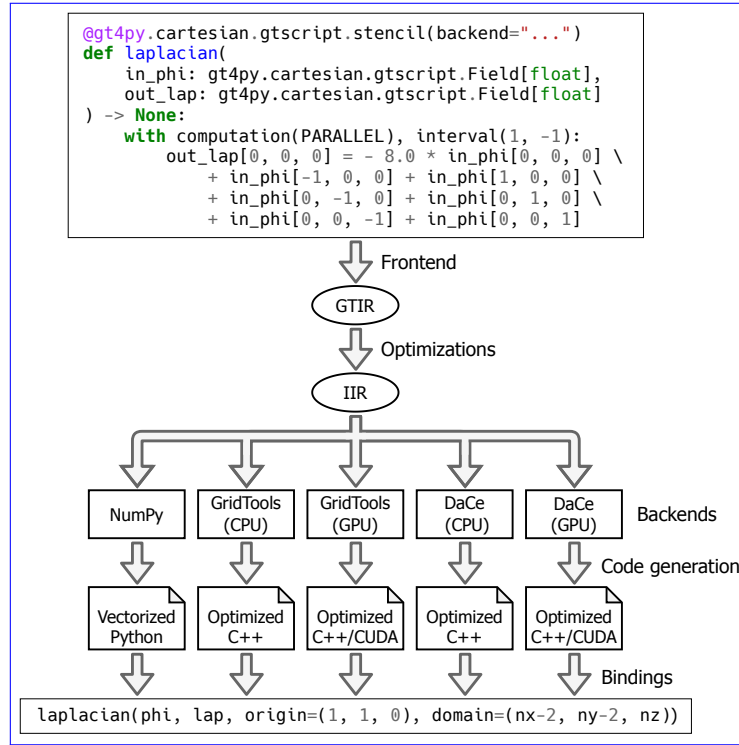


**Figure 2.** Simplified view on the internal stages carried out by the GT4Py toolchain to generate a high-performance CPU or GPU implementation of the ~~horizontal~~ three-dimensional Laplacian stencil starting from its GTScript definition. For the sake of visualization, only two intermediate representations (IRs) are included: the GridTools IR (GTIR) and the Implementation IR (IIR).

accessed through relative offsets, with the first two offsets being the horizontal offsets, and the last offset being the vertical offset.

Any function marked with the `gt4py.cartesian.gtscript.stencil` decorator is translated by the GT4Py *frontend* into a hierarchy of tree-like Intermediate Representations (IRs), featuring different levels of abstractions to accommodate diverse optimizations and transformations (Gysi et al., 2021). The lowest-level IR (denoted as Implementation IR, or IIR) is consumed by the *backends* to generate code that is either optimized for a given architecture or suited to a specific purpose. The following backends are currently available:

- NumPy (Harris et al., 2020) is the *de facto* standard for array computing in Python, and can be used for debugging and fast-prototyping;
- GridTools (Afanasyev et al., 2021) is a set of libraries and utilities to write performance-portable applications in the area of weather and climate;

- DaCe (Ben-Nun et al., 2019) is a parallel programming framework, which internally uses the Stateful DataFlow multiGraph (SDFG) data-centric intermediate representation to decouple domain science and performance engineering.

235 The generated code is compiled under the hood, and Python bindings for the resulting executable are automatically produced, so that the stencil can finally be executed by passing the input and output fields and by specifying the origin and size of the computation domain. GT4Py provides convenient utilities to allocate arrays with an optimal memory layout for any given backend, relying on NumPy for CPU storages and CuPy (Nishino and Loomis, 2017) for GPU storages. Concerning GPU computing, we highlight that GT4Py supports both NVIDIA and AMD GPUs.

240 A more realistic and pertinent code sample is provided in Listing 1. It is an abridged GT4Py implementation of the procedure computing the saturation water vapor pressure as a function of air pressure and temperature. The code is extracted from the CLOUDSC2-GT4Py dwarf and highlights two additional features of GTScript: functions and external symbols. Functions can be thought of as macros, and can be used to improve composability, reusability and readability. External symbols are used to encode those scalar parameters (e.g. physical constants) that are kept

245 constant throughout a simulation, and might only change between different model setups. External values must be provided at stencil compilation time. The functionalities provided by the package `ifs_physics_common` will be discussed in the following section.

## 4 Infrastructure code

All stencils of CLOUDSC-GT4Py and CLOUDSC2-GT4Py are defined, compiled and invoked within classes that

250 leverage the functionalities provided by the Sympl package (Monteiro et al., 2018). Sympl is a toolset of Python utilities to write self-contained and self-documented model components. Because the components share a common Application Public Interface (API), they favor modularity, composability and inter-operability (Schär et al., 2019). These aspects are of utter importance, for instance, when it comes to assessing the impact of process coupling on weather forecasts and climate projections (Ubbiali et al., 2021).

255 Sympl components interact through dictionaries whose keys are the names of the model variables (fields), and whose values are xarray’s `DataArrays` (Hoyer and Hamman, 2017) collecting the grid point values, the labelled dimensions, the axis coordinates, and the units for those variables. The most relevant component exposed by Sympl is `TendencyComponent`, producing tendencies for prognostic variables and retrieving diagnostics. The class defines a

**Listing 1** GTScript (the Python-embedded DSL exposed by GT4Py) functions and stencil computing the saturation water vapor pressure given the air pressure and temperature. Abridged excerpt from the CLOUDSC2-GT4Py dwarf.

---

```

@gt4py.cartesian.gtscript.function
def \DIFdelbegin \DIFdel{foealfcu}\DIFdelend \DIFaddbegin \DIFadd{foealfa}\DIFaddend (t):
    from __externals__ import \DIFdelbegin \DIFdel{RTICECU}\DIFdelend \DIFaddbegin \DIFadd{RTICE}\DIFaddend
    return min(1.0, ((\DIFdelbegin \DIFdel{RTICECU}\DIFdelend \DIFaddbegin \DIFadd{RTICE}\DIFaddend ,

@gt4py.cartesian.gtscript.function
def foeewmcu(t):
    from __externals__ import R2ES, R3IES, R3LES, R4IES, R4LES, RTT
    return R2ES * (
        foealfcu(t) * exp(R3LES * (t - RTT) / (t - R4LES))
        + (\DIFdelbegin \DIFdel{1 }\DIFdelend \DIFaddbegin \DIFadd{1.0 }\DIFaddend - foealfcu(t)) * (exp(

)

@ifs_physics_common.framework.stencil.stencil_collection("saturation")
def saturation(
    in_ap: gtscript.Field[float], in_t: gtscript.Field[float], out_qsat: gtscript.Field[float]
):
    from __externals__ import LPHYLIN, QMAX, R2ES, R3IES, R3LES, R4IES, R4LES, RETV, RTT
    with computation(PARALLEL), interval(...):
        if LPHYLIN: # linearized physics
            alfa = foealfa(in_t)
            foeewl = R2ES * exp(R3LES * (in_t - RTT) / (in_t - R4LES))
            foeewi = R2ES * exp(R3IES * (in_t - RTT) / (in_t - R4IES))
            foeew = alfa * foeewl + (\DIFdelbegin \DIFdel{1 }\DIFdelend \DIFaddbegin \DIFadd{1.0 }\DIFaddend
            qs = min(foeew / in_ap, QMAX)
        else:
            ew = foeewmcu(in_t)
            qs = min(ew / in_ap, QMAX)
        out_qsat[0, 0, 0] = qs / (1.0 - RETV * qs)

```

---

minimal interface to declare the list of input and output fields, and initialize and run an instance of the class. This  
260 imposes minor constraints on model developers when writing a new physics package.

The bespoke infrastructure code for CLOUDSC-GT4Py and CLOUDSC2-GT4Py is bundled as an installable Python package called `ifs_physics_common`. Not only ~~it builds~~ does it build upon Sympl, but ~~is~~ also extends it with grid-aware and stencil-oriented functionalities. Both the CLOUDSC cloud microphysics and the non-linear, tangent-linear and adjoint formulations of CLOUDSC2 are encoded as stand-alone `TendencyComponent` classes  
265 settled over a `ComputationalGrid`. The latter is a collection of index spaces for different grid locations. For instance, (I, J, K) corresponds to cell centers, while (I, J, K-1/2) denotes vertically-staggered grid points. For any input and output field, its name, units and grid location are specified as class properties. When running the component via

---

**Listing 2** A Python class to compute the saturation water vapor pressure given the air pressure and temperature. Abridged excerpt from the CLOUDSC2-GT4Py dwarf.

---

```

import copy as cp
from functools import cached_property
import numpy as np
from typing import Optional, Union
from ifs_physics_common.framework.components import DiagnosticComponent
from ifs_physics_common.framework.config import GT4PyConfig
from ifs_physics_common.framework.grid import ComputationalGrid, I, J, K

# type alias originally defined in ifs_physics_common.utils.typingx
StorageDict = dict[str, Union[cp.ndarray, np.ndarray]]

class Saturation(DiagnosticComponent):
    def __init__(
        self,
        computational_grid: ComputationalGrid,
        lphylin: bool,
        yoethf_parameters: Optional[dict[str, float]] = None,
        yomcst_parameters: Optional[dict[str, float]] = None,
        gt4py_config: GT4PyConfig,
    ) -> None:
        super().__init__(computational_grid, gt4py_config)
        externals = {"LPHYLIN": lphylin, "QMAX": 0.5}
        externals.update(yoethf_parameters or {})
        externals.update(yomcst_parameters or {})
        self.saturation = self.compile_stencil("saturation", externals)

    @cached_property
    def _input_properties(self):
        return {"ap": {"grid": (I, J, K), "units": "Pa"}, "t": {"grid": (I, J, K), "units": "K"}}

    @cached_property
    def _diagnostic_properties(self):
        return {"qsat": {"grid": (I, J, K), "units": "g g-1"}}

    def array_call(self, state: StorageDict, out: StorageDict) -> None:
        self.saturation(
            in_ap=state["ap"],
            in_t=state["t"],
            out_qsat=out["qsat"],
            origin=(0, 0, 0),
            domain=self.computational_grid.grids[I, J, K].shape,
        )

```

---

the *dunder* method `__call__`, Sympl transparently extracts the raw data from the input `DataArrays` according to the information provided in the class definition. This step may involve units conversion and axis transposition. The  
270 resulting storages are forwarded to the method `array_call`, which carries out the actual computations, possibly by executing GT4Py stencil kernels.

Listing 2 brings a concrete example from CLOUDSC2-GT4Py: a model component leveraging the stencil defined in Listing 1 to compute the saturation water vapor pressure. The class inherits `DiagnosticComponent`, a stripped-down version of `TendencyComponent`, which only retrieves diagnostic quantities. Within the instance initializer `__init__`, the  
275 stencil from Listing 1, registered using the decorator `ifs_physics_common.framework.stencil.stencil_collection`, is compiled using the utility method `compile_stencil`. The options configuring the stencil compilation (e.g. the GT4Py backend) are fetched from the dataclass `GT4PyConfig`.

## 5 Performance analysis

In this section, we highlight the results from a comprehensive performance testing. We compare the developed  
280 CLOUDSC-GT4Py and CLOUDSC2-GT4Py codes against reference Fortran versions and various other programming prototypes. The simulations were performed on three different supercomputers:

- (i) Piz Daint<sup>9</sup>, an HPE Cray XC40/XC50 system installed at CSCS in Lugano, Switzerland;
- (ii) MeluXina<sup>10</sup>, an ATOS BullSequana XH2000 machine hosted by LuxConnect in Bissen, Luxembourg, and procured by the EuroHPC Joint Undertaking (JU) initiative;
- 285 (iii) the Cray HPE EX235a supercomputer LUMI<sup>11</sup>, an EuroHPC pre-exascale machine at the Science Information Technology Center (CSC) in Kajaani, Finland.

On each machine, the CLOUDSC and CLOUDSC2 applications are executed on a single hybrid node, that sports one or multiple GPU accelerators alongside the host CPU. An overview of the node architectures for the three considered supercomputers can be found in Table 1.

290 Besides the GT4Py codes, we involve up to four alternative lower-level programming implementations, which will be documented in an upcoming publication.

- (a) The baseline Fortran version, enriched with OpenMP directives for multi-threading execution on CPU.

---

<sup>9</sup><https://www.cscs.ch/computers/piz-daint>

<sup>10</sup><https://docs.lxp.lu/>

<sup>11</sup><https://docs.lumi-supercomputer.eu/>

System	CPU	GPU	RAM	NUMA domains
Piz Daint	1x Intel Xeon E5-2690v3 12c	1x NVIDIA Tesla P100 16GB	64 GB	1
MeluXina	2x AMD EPYC Rome 7452 32c	4x NVIDIA Tesla A100 40GB	512 GB	4
LUMI	1x AMD EPYC Trento 7A53 64c	4x AMD Instinct MI250X	512 GB	8

**Table 1.** Overview of the node architecture for the hybrid partition of Piz Daint, MeluXina and LUMI. Only the technical specifications which are most relevant for the purposes of this paper are reported.

(b) An optimized GPU-enabled version based on OpenACC using the single-column coalesced (SCC) loop layout in combination with loop fusion and temporary local array demotion (so-called “k-caching”). While the SCC loop layout yields more efficient access to device memory and increased parallelism, the k-caching technique significantly reduces register pressure and memory traffic. This is achieved via loop fusion to eliminate most loop-carried dependencies and consequently allows to demote temporaries to scalars.

(c) The currently best-performing Loki generated and GPU-enabled variant.

(d) An optimized GPU-enabled version of CLOUDSC including k-caching. The code is written either in CUDA or HIP, to target both NVIDIA GPUs (shipped with Piz Daint and MeluXina) and AMD GPUs (available on LUMI).

Table 2 documents the compiler specifications employed for each of the programming implementations, on Piz Daint, MeluXina and LUMI. We consistently apply the most aggressive optimization, ensuring that the underlying code manipulations do not harm validation. For the different algorithms at consideration, validation is carried out as follows.

- For CLOUDSC and CLOUDSC2NL, the results from each coding version are directly compared with serialized reference data produced on the CPU. For each output field, we perform an element-wise comparison using the NumPy function `allclose`<sup>12</sup>. Specifically, the GT4Py rewrites `validate` on both CPU and GPU with an absolute and relative tolerance of  $10^{-12}$  and  $10^{-18}$  when employing double precision. When reducing the precision to 32-bits, the absolute and relative tolerance levels need to be increased to  $10^{-4}$  and  $10^{-7}$  on CPU, and  $10^{-2}$  and  $10^{-7}$  on GPU. In the latter case, we observe that the field representing the enthalpy flux of ice still does not pass validation. We attribute the larger deviation from the baseline data on the device to the different instruction sets underneath CPUs and GPUs.

<sup>12</sup><https://numpy.org/devdocs/reference/generated/numpy.allclose.html>

	Implementation	CLOUDSC	CLOUDSC2: Non-linear	CLOUDSC2: Symmetry test
Piz Daint	Fortran: OpenMP (CPU)	Intel Fortran 2021.3.0	Intel Fortran 2021.3.0	Intel Fortran 2021.3.0
	Fortran: OpenACC (GPU)	NVIDIA Fortran 21.3-0	-	-
	Fortran: Loki (GPU)	NVIDIA Fortran 21.3-0	NVIDIA Fortran 21.3-0	-
	C: CUDA (GPU)	NVIDIA CUDA 11.2.67	-	-
	GT4Py: CPU k-first	g++ (GCC) 10.3.0	g++ (GCC) 10.3.0	g++ (GCC) 10.3.0
	GT4Py: DaCe (GPU)	NVIDIA CUDA 11.2.67	NVIDIA CUDA 11.2.67	NVIDIA CUDA 11.2.67
MeluXina	Fortran: OpenMP (CPU)	NVIDIA Fortran 22.7-0	NVIDIA Fortran 22.7-0	-
	Fortran: OpenACC (GPU)	NVIDIA Fortran 22.7-0	-	-
	Fortran: Loki (GPU)	NVIDIA Fortran 22.7-0	NVIDIA Fortran 22.7-0	-
	C: CUDA (GPU)	NVIDIA CUDA 11.7.64	-	-
	GT4Py: CPU k-first	g++ (GCC) 11.3.0	g++ (GCC) 11.3.0	g++ (GCC) 11.3.0
	GT4Py: DaCe (GPU)	NVIDIA CUDA 11.7.64	NVIDIA CUDA 11.7.64	NVIDIA CUDA 11.7.64
LUMI	Fortran: OpenMP (CPU)	Cray Fortran 14.0.2	Cray Fortran 14.0.2	Cray Fortran 14.0.2
	Fortran: OpenACC (GPU)	Cray Fortran 14.0.2	-	-
	Fortran: Loki (GPU)	Cray Fortran 14.0.2	Cray Fortran 14.0.2	-
	C: HIP (GPU)	Cray C/C++ 15.0.1	-	-
	GT4Py: CPU k-first	Cray C/C++ 15.0.1	Cray C/C++ 15.0.1	Cray C/C++ 15.0.1
	GT4Py: DaCe (GPU)	Cray C/C++ 15.0.1	Cray C/C++ 15.0.1	Cray C/C++ 15.0.1

**Table 2.** For each coding version of the CLOUDSC and CLOUDSC2 dwarfs considered in the performance analysis, the table reports the compiler suite used to compile the codes on Piz Daint, MeluXina and LUMI. The codes are compiled with all major optimization options enabled. Those implementations which are either not available or not working are marked with a dash; more details, as well as a high-level description of each coding implementation, are provided in the text.

– All implementations of CLOUDSC2TL and CLOUDSC2AD are validated using the Taylor test (cf. Algorithm A1) and the symmetry test (cf. Algorithm A2), respectively. ~~However, the~~ In this respect, we emphasize that the GT4Py implementations satisfy the conditions of both tests ~~are not satisfied when using single precision~~. ~~This is not surprising, since both tests are highly sensitive to round-off errors. Nevertheless, performance numbers for the execution of the algorithms were taken.~~ on all considered computing architectures, regardless of whether double or single precision is employed.

The source repositories for CLOUDSC and CLOUDSC2 dwarfs may include multiple variants of each reference implementation, varying for the optimization strategies. In our analysis, we always take into account the fastest variant of each alternative implementation; for the sake of reproducibility, Table 3 contains the strings identifying the coding versions at consideration and the corresponding NPROMA<sup>13</sup> employed in the runs. Similarly, for all Python

<sup>13</sup>NPROMA slicing is a cache blocking technique adopted in all Fortran codes considered in this paper. Given a two-dimensional array shaped  $(K * M, N)$ , this is re-arranged as a three-dimensional array shaped  $(K, M, N)$ . The leading dimension of the three-dimensional array is commonly called “NPROMA”, with  $K$  being the “NPROMA blocking factor”. For the sake of brevity, in the text we indicate  $K$



	Implementation	CLOUDSC	CLOUDSC2: Non-linear	CLOUDSC2: Symmetry test
Piz Daint	Fortran: OpenMP (CPU)	fortran (32)	nl (32)	ad (32)
	Fortran: OpenACC (GPU)	gpu-scc-k-caching (128)	-	-
	Fortran: Loki (GPU)	loki-scc-cuf-hoist (128)	nl-loki-scc-hoist (64)	-
	C: CUDA (GPU)	cuda-k-caching (128)	-	-
MeluXina	Fortran: OpenMP (CPU)	fortran (32)	nl (32)	-
	Fortran: OpenACC (GPU)	gpu-scc-k-caching (128)	-	-
	Fortran: Loki (GPU)	loki-scc-cuf-hoist (128)	nl-loki-scc-hoist (128)	-
	C: CUDA (GPU)	cuda-k-caching (128)	-	-
LUMI	Fortran: OpenMP (CPU)	fortran (32)	nl (32)	ad (32)
	Fortran: OpenACC (GPU)	gpu-scc-k-caching (256)	-	-
	Fortran: Loki (GPU)	loki-scc-hoist (256)	nl-loki-scc-hoist (256)	-
	C: HIP (GPU)	hip-k-caching (64)	-	-

**Table 3.** For each reference implementation of the CLOUDSC and CLOUDSC2 dwarfs, the table reports the string identifying the specific variant considered in the performance analysis on Piz Daint, MeluXina and LUMI. The corresponding NPROMA is provided within parentheses. Those implementations which are either not available or not working are marked with a dash.

implementations we consider only the most performant backends of GT4Py: the GridTools C++ CPU backend with  
 325 k-first memory layout, and the DaCe GPU backend.

For the interpretation of the CPU versus GPU performance numbers, we note that host codes are executed on all the  
 cores available on a single Non-Uniform Memory Access (NUMA) domain of a compute node, while device codes are  
 launched on the GPU attached to that NUMA domain. In a distributed-memory context, this choice allows to fit the  
 same number of MPI ranks per node, either on CPU or GPU. Table 1 reports the number of NUMA partitions per  
 330 node for Piz Daint, MeluXina and LUMI, with the compute and memory resources being evenly distributed across  
 the NUMA domains. Note that the compute nodes of the GPU partition of LUMI have the low-noise mode activated,  
 which reserves one core per NUMA domain to the operating system, so that only 7 out of 8 cores are available to the  
 jobs. Moreover, we highlight that each MI250X GPU ~~is split into two~~ consists of two Graphics Compute Dies (GCDs)  
 connected via four AMD Infinity Fabric links but not sharing physical memory. From a software perspective, each  
 335 compute node of LUMI is equipped with 8 virtual GPUs (vGPUs), with each vGPU corresponding to a single GCD  
 and assigned to a different NUMA domain.

Figures 3-5 visualize the execution times for CLOUDSC (left column), CLOUDSC2NL (center column) and  
 the symmetry test for CLOUDSC2TL and CLOUDSCAD (right column) for Piz Daint, MeluXina and LUMI,

---

simply as “NPROMA”. For an insightful discussion on the NPROMA slicing technique, we refer the readers to, e.g., Müller et al. (2019)  
 and Bauer et al. (2020).

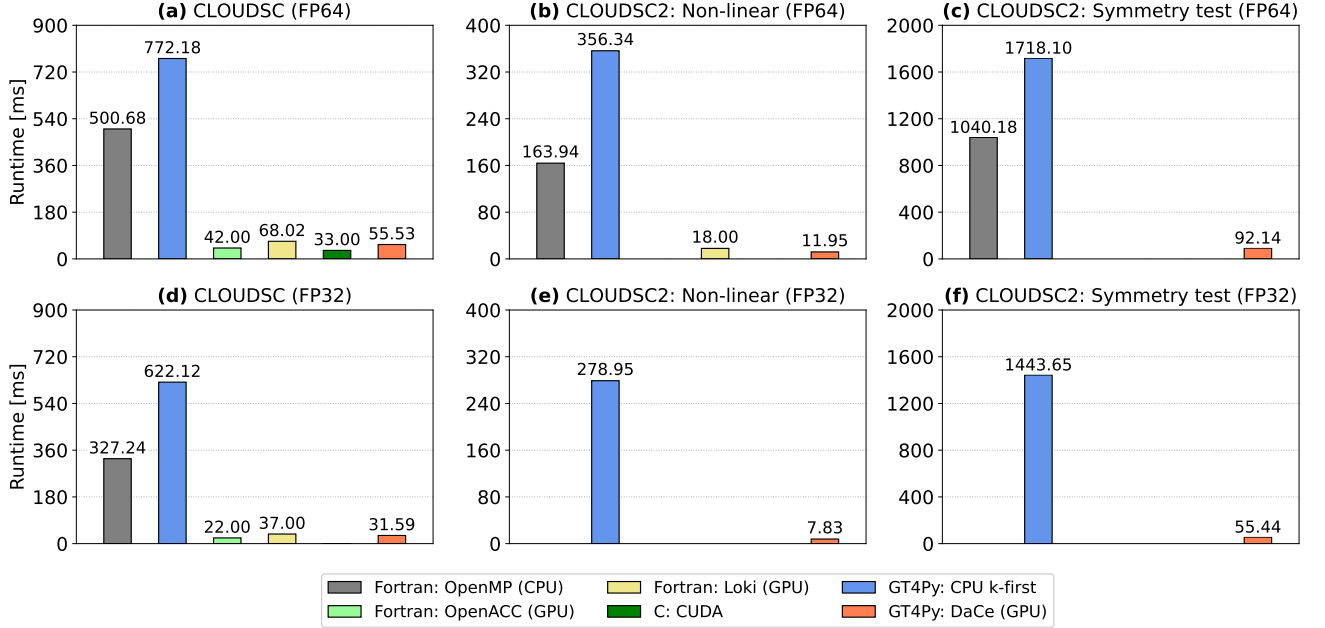


**Figure 3.** Execution time on a single NUMA domain of a hybrid node of the Piz Daint supercomputer for CLOUDSC (left column), CLOUDSC2NL (center column) and the symmetry test for CLOUDSC2TL and CLOUDSC2AD (right column) using either double precision (top row) or single precision (bottom row) floating point arithmetic. The computational domain consists of 65536 columns and 137 vertical levels. Displayed are the multi-threaded Fortran baseline using OpenMP (grey); two GPU-accelerated Fortran implementations, either using OpenACC directives (lime) or the source-to-source translation tool Loki (yellow); an optimized CUDA C version (green); and the GT4Py rewrite, either using the GridTools C++ CPU backend with k-first data ordering (blue) or the DaCe GPU backend (orange). All numbers should be interpreted as an average over 50 realizations. The panels only show the code versions available and validating at the time of writing.

respectively<sup>14</sup>. All performance numbers refer to a grid size of 65536 columns, with each column featuring 137 vertical levels. In each figure, execution times are provided for simulations running either entirely in double precision (corresponding to the 64-bit IEEE format and denoted as FP64; top row) or in single precision (corresponding to the 32-bit IEEE format and denoted as FP32; bottom row). Within each panel, the plotted bars reflect the execution time of the various codes, with a missing bar indicating the corresponding code (non-GT4Py) is either not available or not working properly. Specifically,

- the Fortran version of CLOUDSC2AD can only run on a single OpenMP thread on MeluXina (the issue is still under investigation);

<sup>14</sup>When measuring the performance of the symmetry test, the validation procedure – corresponding to lines 11-23 of Algorithm A2 – is switched off.

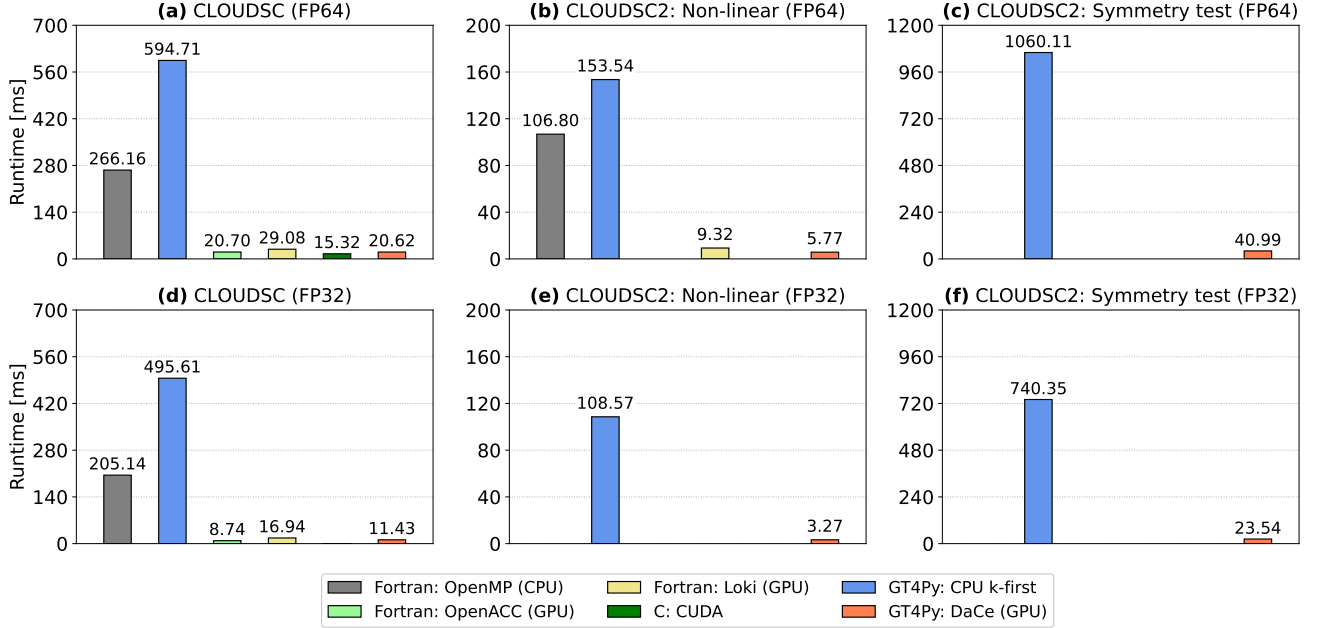


**Figure 4.** As Fig. 3 but for the MeluXina supercomputer.

- a native GPU-enabled version of CLOUDSC using 32-bit floating point arithmetic does not exist at the time of writing, and no CUDA/HIP implementations are available for CLOUDSC2;
- all Fortran-based implementations of the three formulations of CLOUDSC2 can only use double precision computations;
- a Loki version of CLOUDSC2TL and CLOUDSC2AD is not available at the time of writing.

Notably, we find the GT4Py rewrite of both CLOUDSC and CLOUDSC2 to be very robust, as the codes execute on every CPU and GPU architecture included in the study, and can always employ either double or single precision floating point arithmetic. With GT4Py, changing the backend with the respective target architecture, or changing the precision of computations, is as easy as setting a namelist parameter. Moreover, at the time of writing the GT4Py implementations of the more complex tangent-linear and adjoint formulations of CLOUDSC2 were the first codes enabling GPU execution, again both in double or single precision.

The performance of the high-level Python with GT4Py compares well against Fortran with OpenACC. The runtimes for GT4Py with its DaCe backend versus OpenACC are similar on Piz Daint, MeluXina and LUMI. One outlier is the double precision result on LUMI, for which the OpenACC code appears relatively slow. We suppose

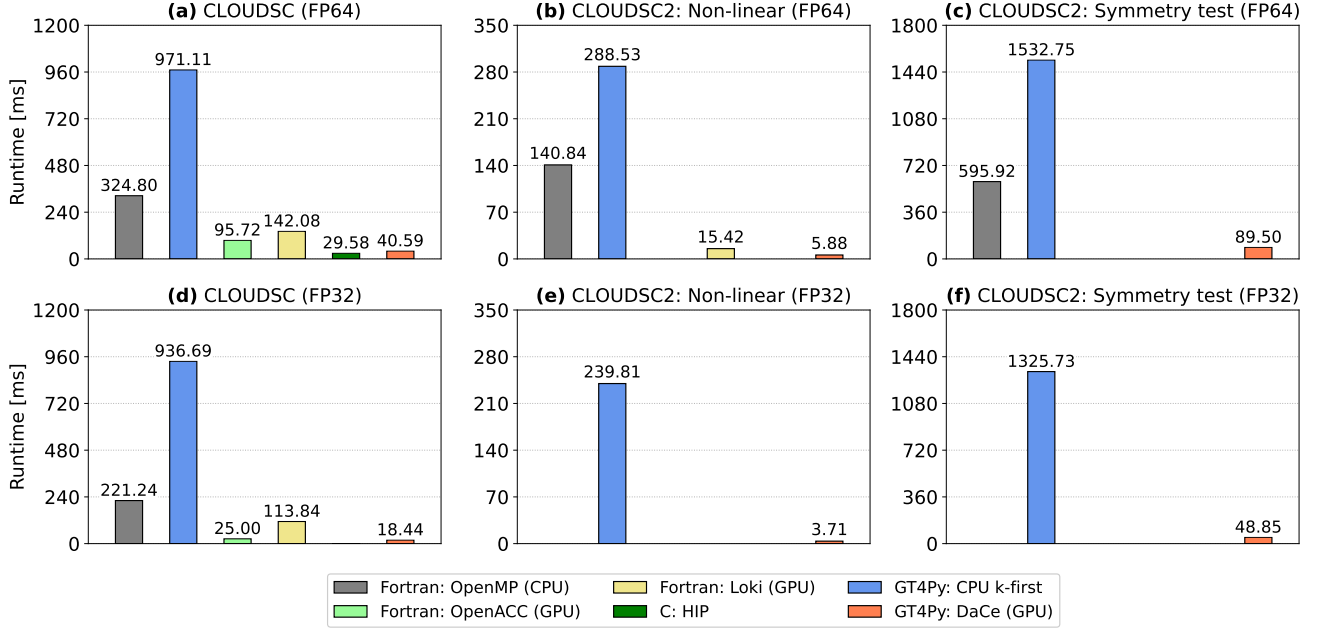


**Figure 5.** As Fig. 3 but for the LUMI supercomputer.

this behaviour is associated with the insufficient OpenACC support for the HPE Cray compiler. Only the HPE Cray compiler implements GPU offloading capabilities for OpenACC directives on AMD GPUs, meaning that Fortran OpenACC codes require an HPE Cray platform to run on AMD GPUs. In contrast, GT4Py relies on the HIPCC compiler driver developed by AMD to compile device code for AMD accelerators, and this guarantees a proper functioning irrespective of the machine vendor. We further note that the DaCe backend of GT4Py executes roughly two times faster on MeluXina’s NVIDIA A100 GPUs than on LUMI’s AMD Instinct MI250X GPUs. As mentioned above, from a software perspective, each physical GPU module on LUMI is considered as two virtual GPUs, so that the code is actually executed on half of a physical GPU card. We can therefore speculate that if using both dies of an AMD Instinct MI250X GPU performance would be on par with the NVIDIA A100 GPU.

Another interesting result is that both CLOUDSC-GT4Py and CLOUDSC2-GT4Py are consistently faster than the implementations generated with Loki. Loki allows to build bespoke transformation recipes to apply changes to programming models and coding styles in an automated fashion. Therefore, GPU-enabled code can be produced starting from the original Fortran by e.g., automatically adding OpenACC directives. However, because not all optimizations are yet encoded in the transformations, the Loki-generated device code cannot achieve optimal

375 performance. Notwithstanding, source-to-source translators such as Loki are of high relevance for enabling GPU execution with large legacy Fortran code bases.

As used in this paper, GT4Py cannot yet attain the performance achieved by manually optimized native implementations with either Fortran on CPU or CUDA/HIP on GPU. Multi-threaded Fortran can be up to three times faster than the GridTools CPU backend of GT4Py using the k-first (C-like) memory layout, while the DaCe GPU backend  
380 of GT4Py can be up to a factor of two slower than CUDA/HIP. On the one hand, so far the development of GT4Py has been focused on GPU execution (see e.g. Dahm et al. (2023)), because this will be the dominant hardware for time-critical applications in the years to come. On the other hand, we stress that the k-caching CUDA and HIP variants of CLOUDSC were semi-automatically generated by performance engineering experts, starting from an automatic Fortran-to-C transpilation of the SCC variants and manually applying additional optimizations that require  
385 knowledge about the specific compute patterns in the application. This process is not scalable to the full weather model and not a sustainable code adaptation method. In contrast, no significant performance engineering ([by e.g., statements fusion and temporaries pruning](#)) has been applied yet with CLOUDSC-GT4Py and CLOUDSC2-GT4Py.

To rule out the possibility that the performance gap between the Python DSL and lower-level codes is associated with overhead originating from Python, Fig. 6 displays the fraction of runtime spent within the stencil code generated  
390 by GT4Py and the high-level Python code of the application (infrastructure and framework code; see Section 4). Across the three supercomputers, the Python overhead decreases as (i) the complexity and length of computations increase, (ii) the peak throughput and bandwidth delivered by the hardware underneath decrease, and (iii) the floating point precision increases. On average, the Python overhead accounts for 5.4% of the total runtime on GPU and 0.4% on CPU. [Interestingly, if one takes into account only the cases for which a working Fortran CPU implementation is available, even if the GT4Py performance was on par with Fortran, the Python overhead would still amount to less](#)  
395 [than 0.7% of the total execution time on average.](#)

Finally, we observe a significant sensitivity of the GPU performance with respect to the thread block size<sup>15</sup>: for values smaller than 128, performance is degraded across all implementations, with the gap between CUDA/HIP and GT4Py+DaCe being smaller. This shows that some tuning and toolchain optimizations can be performed to improve  
400 performance with the DSL approach.

---

<sup>15</sup>In the Fortran code, the thread block size corresponds to the NPROMA.

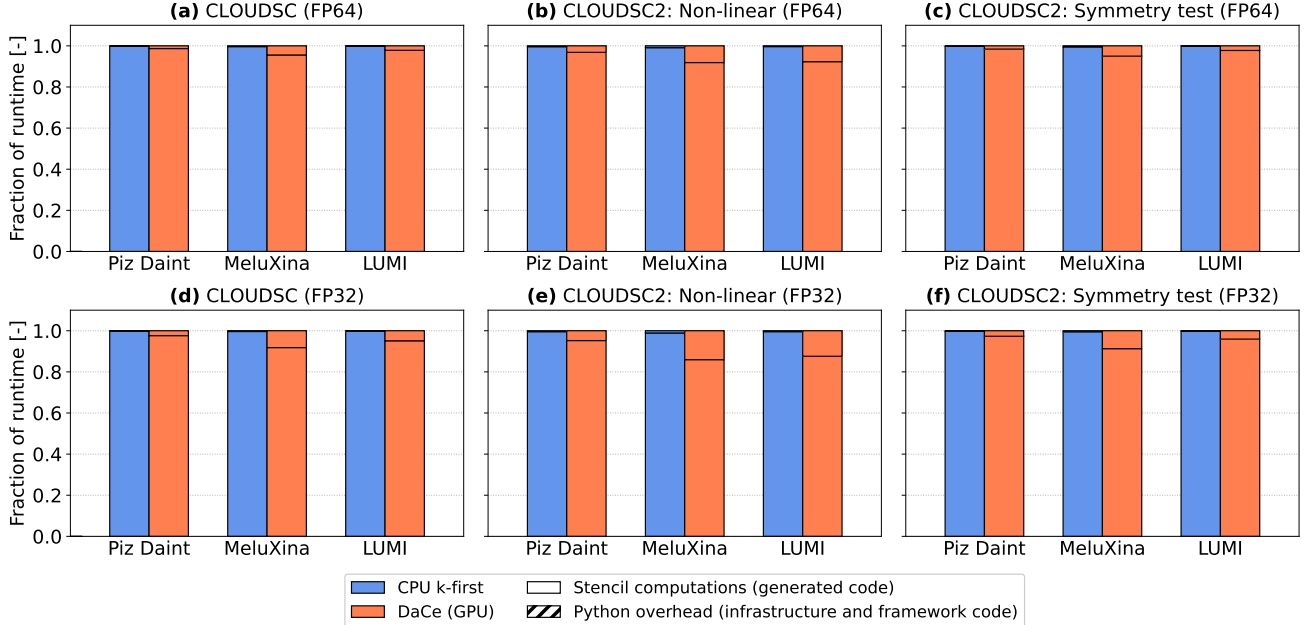


**Figure 6.** For the GT4Py rewrites of CLOUDSC (left column), CLOUDSC2NL (center column) and the symmetry test for CLOUDSC2TL and CLOUDSC2AD (right column), fraction of the total execution time spent within the stencil computations (full bars) and the Python side of the application (hatched bars) on Piz Daint, MeluXina and LUMI. Results are shown for the GridTools C++ CPU backend with k-first data ordering (blue) and the DaCe GPU backend (orange), either using double precision (top row) or single precision (bottom row) floating point arithmetic.

## 6 Conclusions

The CLOUDSC and CLOUDSC2 cloud microphysics schemes of the IFS at ECMWF have served as demonstrators to show the benefits of a high-level domain-specific implementation approach to physical parametrizations. We presented two Python implementations based on the GT4Py framework, in which the scientific code is insulated from hardware-specific aspects. The resulting application provides a productive user interface with enhanced readability and maintainability, and can run efficiently and in a very robust manner across a wide spectrum of compute architectures/systems. The approach can be powerful in the light of the increasingly complex HPC technology landscape, where general-purpose CPUs are increasingly complemented by domain-specific architectures (DSAs) such as GPUs, Tensor Processor Units (TPUs), Field Programmable Gate Arrays (FPGAs), and Application-Specific Integrated Circuits (ASICs). In addition to the CLOUDSC scheme used in the IFS forecast model, we have presented results with the GT4Py rewrites of the nonlinear, tangent-linear and adjoint formulations of CLOUDSC2 used in data assimilation.

In both CLOUDSC-GT4Py and CLOUDSC2-GT4Py, the stencil kernels are encapsulated within model components sharing a minimal and clear interface. By avoiding any assumption on the host model, the interface aims to provide  
415 interoperable and plug-and-play physical packages, which can be transferred more easily between different modeling systems with virtually no performance penalty.

We carried out a comprehensive study to assess the portability of the Python codes across three major supercomputers, differing in terms of the vendor, the node architecture, the software stack and the compiler suites. We showed that the GPU performance of GT4Py codes are competitive against optimized Fortran OpenACC implementations  
420 and perform particularly well when compared to the available codes generated with the Loki source-to-source translation tool. Low-level implementations written either in Fortran for CPUs or CUDA/HIP for GPUs, with additional optimizations that possibly require knowledge about the specific compute patterns, can provide better performance, but are extremely challenging to create and maintain for entire models. The CPU performance of GT4Py is currently suboptimal, but this is an expected result given the focus on GPUs in the DSL development so  
425 far and we clearly expect this to improve significantly with upcoming and future GT4Py versions. Indeed, since the DSL can accommodate any specific low-level optimization, attaining the same performance as native Fortran and CUDA/HIP models is feasible and will be the target of our future efforts.

The presented results, based on a representative physical parametrization and considering tangent-linear and adjoint versions, add to the notion that weather and climate model codes can execute significantly faster on GPUs  
430 (Fuhrer et al., 2018), and the number of HPC systems with accelerators is steadily increasing<sup>16</sup>. Therefore, we envision that CPUs will be increasingly relegated to tasks that are not time-critical.

The current study supports our ongoing efforts and plans to port other physical parametrizations to Python with GT4Py. However, we note that GT4Py has been originally devised to express the computational motifs of dynamical cores based on grid-point methods, so not all patterns found in the parametrizations are natively supported by  
435 the DSL. ~~These cases~~ In this respect, the main limitations of the DSL pertain to data dimensions, single column abstractions, and vertical reductions. These deficiencies may be addressed by new features added to GT4Py or by resorting to other Python libraries to generate fast machine code.

## Appendix A: Algorithmic description of the Taylor test and symmetry test for CLOUDSC2

---

<sup>16</sup>In the 62<sup>nd</sup> edition of the TOP500 list published in November 2023, 186 out of the 500 most powerful supercomputers in the world use graphics accelerator technology (<https://www.top500.org/lists/top500/2023/11/highs/>).

In Section 2.2, we briefly described the aim and functioning of the Taylor test and the symmetry test for CLOUDSC2.  
440 Here, we detail the logical steps performed by the two tests with the help of pseudo-codes encapsulated in Algorithms  
A1 and A2.



**Algorithm A1** The Taylor test assessing the formal correctness of the coding implementation of the tangent-linear formulation of CLOUDSC2, denoted as CLOUDSC2TL. The three-dimensional arrays  $\mathbf{x}$  and  $\mathbf{y}$  collect the grid point values for all  $nin$  input fields and  $nout$  output fields of CLOUDSC2, respectively. The corresponding variations are  $\delta\mathbf{x}$  and  $\delta\mathbf{y}$ . The grid consists of  $ncol$  columns, each containing  $nlev$  vertical levels. Note that compared to its functional counterpart  $F'[\mathbf{x}]: \delta\mathbf{x} \mapsto \delta\mathbf{y}$ , CLOUDSC2TL( $\mathbf{x}, \delta\mathbf{x}$ ) returns both  $\mathbf{y}$  and  $\delta\mathbf{y}$ . The coding implementation of the non-linear CLOUDSC2 is indicated as CLOUDSC2NL.

---

```

1: function TOTALNORM( $ncol, nlev, nout, \mathbf{y}, \mathbf{y}_j, \delta\mathbf{y}_j$ )  $\triangleright \mathbf{y}, \mathbf{y}_j, \delta\mathbf{y}_j \in \mathbb{R}^{ncol \times nlev \times nout}$ 
2:    $total\_norm \leftarrow 0$ 
3:    $total\_count \leftarrow 0$ 
4:   for  $l \leftarrow 1$  to  $nout$  do
5:      $\beta \leftarrow \left| \sum_{i=1}^{nlev} \sum_{k=1}^{ncol} \delta\mathbf{y}_j(i, k, l) \right|$ 
6:     if  $\beta > 0$  then
7:        $total\_norm \leftarrow total\_norm + \left| \sum_{i=1}^{nlev} \sum_{k=1}^{ncol} (\mathbf{y}_j(i, k, l) - \mathbf{y}(i, k, l)) \right| / \beta$ 
8:        $total\_count \leftarrow total\_count + 1$ 
9:   if  $total\_count > 0$  then
10:    return  $total\_norm / total\_count$ 
11:   else
12:    return 0

13: procedure TAYLORTEST( $ncol, nlev, nin, nout, \mathbf{x}$ )  $\triangleright \mathbf{x} \in \mathbb{R}^{ncol \times nlev \times nin}$ 
14:    $\delta\mathbf{x} \leftarrow 0.01 * \mathbf{x}$ 
15:    $(\mathbf{y}, \delta\mathbf{y}) \leftarrow \text{CLOUDSC2TL}(\mathbf{x}, \delta\mathbf{x})$   $\triangleright \mathbf{y}, \delta\mathbf{y} \in \mathbb{R}^{ncol \times nlev \times nout}$ 
16:    $norms \leftarrow ()$ 
17:    $jstart \leftarrow 1$ 
18:   for  $j \leftarrow 1$  to 10 do
19:      $\mathbf{y}_j \leftarrow \text{CLOUDSC2NL}(\mathbf{x} + 10^{-j} * \delta\mathbf{x})$ 
20:      $norms \leftarrow norms \cup (1 - \text{TOTALNORM}(ncol, nlev, nout, \mathbf{y}, \mathbf{y}_j, 10^{-j} * \delta\mathbf{y}))$ 
21:     if  $jstart = 1$  &  $norms(j) < 0.5$  then
22:        $jstart \leftarrow j$ 
23:    $test \leftarrow -10$ 
24:    $negat \leftarrow \text{True}$ 
25:   for  $j \leftarrow jstart$  to 9 do
26:     if  $negat$  &  $norms(j+1) \geq norms(j)$  then
27:        $test \leftarrow test + 10$ 
28:      $negat \leftarrow norms(j+1) < norms(j)$ 
29:   if  $test = -10$  then
30:      $test \leftarrow 11$ 
31:   if  $\min_{jstart \leq j \leq 10} (norms(j)) > 10^{-5}$  then
32:      $test \leftarrow test + 7$ 
33:   if  $\min_{jstart \leq j \leq 10} (norms(j)) > 10^{-6}$  then
34:      $test \leftarrow test + 5$ 
35:   if  $test \leq 5$  then
36:     print "The Taylor test passed."
37:   else
38:     print "The Taylor test failed."

```

---

---

**Algorithm A2** The symmetry test assessing the formal correctness of the coding implementation of the adjoint formulation of CLOUDSC2, denoted as CLOUDSC2AD. The machine epsilon is indicated as  $\varepsilon$ ; all other symbols have the same meaning as in Algorithm A1. Note that compared to its functional counterpart  $F^*[F(\mathbf{x})] : \delta\mathbf{y} \mapsto \delta\mathbf{x}^*$ , CLOUDSC2AD( $\mathbf{x}, \delta\mathbf{y}$ ) returns both  $\mathbf{y}$  and  $\delta\mathbf{x}^*$ .

---

```

1: function COLUMNWISEINNERPRODUCT( $ncol, nlev, ndim, \mathbf{a}, \mathbf{b}$ )                                 $\triangleright \mathbf{a}, \mathbf{b} \in \mathbb{R}^{ncol \times nlev \times ndim}$ 
2:    $\mathbf{c} \leftarrow \mathbf{0} \in \mathbb{R}^{ncol}$ 
3:   for  $l \leftarrow 1$  to  $ndim$  do
4:     for  $i \leftarrow 1$  to  $ncol$  do
5:        $\mathbf{c}(i) \leftarrow \mathbf{c}(i) + \sum_{k=1}^{nlev} \mathbf{a}(i, k, l) * \mathbf{b}(i, k, l)$ 
6:   return  $\mathbf{c}$ 

7: procedure SYMMETRYTEST( $ncol, nlev, nin, nout, \mathbf{x}, \varepsilon$ )                                 $\triangleright \mathbf{x} \in \mathbb{R}^{ncol \times nlev \times nin}$ 
8:    $\delta\mathbf{x} \leftarrow 0.01 * \mathbf{x}$ 
9:    $(\mathbf{y}, \delta\mathbf{y}) \leftarrow \text{CLOUDSC2TL}(\mathbf{x}, \delta\mathbf{x})$                                  $\triangleright \mathbf{y}, \delta\mathbf{y} \in \mathbb{R}^{ncol \times nlev \times nout}$ 
10:   $(\mathbf{y}, \delta\mathbf{x}^*) \leftarrow \text{CLOUDSC2AD}(\mathbf{x}, \delta\mathbf{y})$                                  $\triangleright \mathbf{x}^*, \delta\mathbf{x}^* \in \mathbb{R}^{ncol \times nlev \times nin}$ 
11:   $\mathbf{c}_y \leftarrow \text{COLUMNWISEINNERPRODUCT}(ncol, nlev, nout, \delta\mathbf{y}, \delta\mathbf{y})$ 
12:   $\mathbf{c}_x \leftarrow \text{COLUMNWISEINNERPRODUCT}(ncol, nlev, nin, \delta\mathbf{x}, \delta\mathbf{x}^*)$ 
13:   $success \leftarrow \text{True}$ 
14:  for  $i \leftarrow 1$  to  $ncol$  do
15:    if  $\mathbf{c}_x(i) = 0$  then
16:       $c \leftarrow |\mathbf{c}_y(i)| / \varepsilon$ 
17:    else
18:       $c \leftarrow |\mathbf{c}_x(i) - \mathbf{c}_x(i)| / |\varepsilon * \mathbf{c}_x(i)|$ 
19:     $success \leftarrow success \ \& \ c < 10^3$ 
20:  if  $success$  then
21:    print "The symmetry test passed."
22:  else
23:    print "The symmetry test failed."

```

---

*Code and data availability.* The source codes for `ifs-physics-common` (Ubbiali et al., 2024b, <https://github.com/stubbiali/ifs-physics-common>), `CLOUDSC-GT4Py` (Ubbiali et al., 2024c, <https://github.com/stubbiali/gt4py-dwarf-p-cloudsc>) and `CLOUDSC2-GT4Py` (Ubbiali et al., 2024d, <https://github.com/stubbiali/gt4py-dwarf-p-cloudsc2-tl-ad>), as well as the data  
445 and scripts to produce all the figures of the paper (Ubbiali et al., 2024a, <https://github.com/stubbiali/cloudsc-paper>), are available on Github and archived on Zenodo.

*Author contributions.* SU ported the CLOUDSC and CLOUDSC2 dwarfs to Python using GT4Py and ran all the numerical experiments presented in the paper, under the supervision of CK and HW. SU further contributed to the development of the infrastructure code illustrated in Section 4, under the supervision of CS, LS and TCS. MS made relevant contributions to the

450 Fortran and C reference implementations of the ECMWF microphysics schemes. SU and CK wrote the paper, with feedback from all co-authors.

*Competing interests.* The authors declare that they have no conflict of interest.

*Acknowledgements.* We would like to thank three anonymous referees for carefully reviewing the manuscript and providing many constructive comments. This study was conducted as part of the Platform for Advanced Scientific Computing (PASC) funded project KILOS (“Kilometer-scale non-hydrostatic global weather forecasting with IFS-FVM”), which also provided us with computing resources on the Piz Daint supercomputer at CSCS. CK has received funding from the ESiWACE3 project funded by the European High Performance Computing Joint Undertaking (EuroHPC JU) and the European Union (EU) under grant agreement No 101093054. We acknowledge EuroHPC JU for awarding the project ID 200177 access to the MeluXina supercomputer at LuxConnect and the project ID 465000527 access to the LUMI system at CSC, and thank Thomas  
455  
460 Geenen and Nils Wedi from Destination Earth for their help. We are grateful to Michael Lange and Balthasar Reuter for discussions and support regarding IFS codes.

## References

- Adams, S. V., Ford, R. W., Hambley, M., Hobson, J., Kavčič, I., Maynard, C. M., Melvin, T., Müller, E. H., Mullerworth, S.,  
Porter, A., et al.: LFRic: Meeting the challenges of scalability and performance portability in Weather and Climate models,  
465 Journal of Parallel and Distributed Computing, 132, 383–396, <https://doi.org/10.1016/j.jpdc.2019.02.007>, 2019.
- Afanasyev, A., Bianco, M., Mosimann, L., Osuna, C., Thaler, F., Vogt, H., Fuhrer, O., VandeVondele, J., and  
Schulthess, T. C.: GridTools: A framework for portable weather and climate applications, SoftwareX, 15, 100 707,  
<https://doi.org/10.1016/j.softx.2021.100707>, 2021.
- Baldauf, M., Seifert, A., Förstner, J., Majewski, D., Raschendorfer, M., and Reinhardt, T.: Operational convective-scale  
470 numerical weather prediction with the COSMO model: Description and sensitivities, Monthly Weather Review, 139,  
3887–3905, <https://doi.org/10.1175/mwr-d-10-05013.1>, 2011.
- Bauer, P., Quintino, T., Wedi, N., Bonanni, A., Chrust, M., Deconinck, W., Diamantakis, M., Düben, P., English, S., Flemming,  
J., et al.: The ECMWF scalability programme: Progress and plans, ECMWF Technical Memo No. 857, 2020.
- Bauer, P., Dueben, P. D., Hoefer, T., Quintino, T., Schulthess, T. C., and Wedi, N. P.: The digital revolution of Earth-system  
475 science, Nature Computational Science, 1, 104–113, <https://doi.org/10.1038/s43588-021-00023-0>, 2021.
- Ben-Nun, T., de Fine Licht, J., Ziogas, A. N., Schneider, T., and Hoefer, T.: Stateful Dataflow Multigraphs: A Data-Centric  
Model for Performance Portability on Heterogeneous Architectures, in: Proceedings of the International Conference for High  
Performance Computing, Networking, Storage and Analysis, SC ’19, <https://doi.org/10.1145/3295500.3356173>, 2019.
- Ben-Nun, T., Groner, L., Deconinck, F., Wicky, T., Davis, E., Dahm, J., Elbert, O. D., George, R., McGibbon, J.,  
480 Trümper, L., et al.: Productive performance engineering for weather and climate modeling with Python, in: SC22:  
International Conference for High Performance Computing, Networking, Storage and Analysis, pp. 1–14, IEEE,  
<https://doi.org/10.1109/sc41404.2022.00078>, 2022.
- Bertagna, L., Guba, O., Taylor, M. A., Foucar, J. G., Larkin, J., Bradley, A. M., Rajamanickam, S., and Salinger, A. G.:  
A performance-portable nonhydrostatic atmospheric dycore for the Energy Exascale Earth System Model running at  
485 cloud-resolving resolutions, in: SC20: International Conference for High Performance Computing, Networking, Storage and  
Analysis, pp. 1–14, IEEE, <https://doi.org/10.2172/1830973>, 2020.
- Chandrasekaran, S. and Juckeland, G.: OpenACC for Programmers: Concepts and Strategies, Addison-Wesley Professional,  
2017.
- Clement, V., Marti, P., Lapillonne, X., Fuhrer, O., and Sawyer, W.: Automatic Port to OpenACC/OpenMP for Physical  
490 Parameterization in Climate and Weather Code Using the CLAW Compiler, Supercomputing Frontiers and Innovations, 6,  
51–63, <https://doi.org/10.14529/jsfi190303>, 2019.

- Courtier, P., Thépaut, J.-N., and Hollingsworth, A.: A strategy for operational implementation of 4D-Var, using an incremental approach, *Quarterly Journal of the Royal Meteorological Society*, 120, 1367–1387, <https://doi.org/10.1256/smsqj.51911>, 1994.
- 495 Dagum, L. and Menon, R.: OpenMP: an industry standard API for shared-memory programming, *IEEE Computational Science and Engineering*, 5, 46–55, <https://doi.org/10.1109/99.660313>, 1998.
- Dahm, J., Davis, E., Deconinck, F., Elbert, O., George, R., McGibbon, J., Wicky, T., Wu, E., Kung, C., Ben-Nun, T., et al.: Pace v0. 2: a Python-based performance-portable atmospheric model, *Geoscientific Model Development*, 16, 2719–2736, <https://doi.org/10.5194/gmd-16-2719-2023>, 2023.
- 500 Deakin, T., McIntosh-Smith, S., Price, J., Poenaru, A., Atkinson, P., Popa, C., and Salmon, J.: Performance portability across diverse computer architectures, in: 2019 IEEE/ACM International Workshop on Performance, Portability and Productivity in HPC (P3HPC), pp. 1–13, IEEE, <https://doi.org/10.1109/p3hpc49587.2019.00006>, 2019.
- ECMWF: IFS Documentation CY48R1 - Part IV: Physical Processes, ECMWF, 2023.
- Edwards, H. C., Trott, C. R., and Sunderland, D.: Kokkos: Enabling manycore performance portability  
505 through polymorphic memory access patterns, *Journal of Parallel Distributed Computing*, 74, 3202–3216, <https://doi.org/10.1016/j.jpdc.2014.07.003>, 2014.
- Errico, R. M.: What is an adjoint model?, *Bulletin of the American Meteorological Society*, 78, 2577–2592, [https://doi.org/10.1175/1520-0477\(1997\)078<2577:WIAAM>2.0.CO;2](https://doi.org/10.1175/1520-0477(1997)078<2577:WIAAM>2.0.CO;2), 1997.
- Forbes, R. M., Tompkins, A. M., and Untch, A.: A new prognostic bulk microphysics scheme for the IFS, ECMWF Technical  
510 Memo. No. 649, 2011.
- Fuhrer, O., Osuna, C., Lapillonne, X., Gysi, T., Cumming, B., Bianco, M., Arteaga, A., and Schulthess, T. C.: Towards a performance portable, architecture agnostic implementation strategy for weather and climate models, *Supercomputing Frontiers and Innovations*, 1, 45–62, <https://doi.org/10.14529/jsf140103>, 2014.
- Fuhrer, O., Chadha, T., Hoefer, T., Kwasniewski, G., Lapillonne, X., Leutwyler, D., Lüthi, D., Osuna, C., Schär, C., Schulthess,  
515 T. C., et al.: Near-global climate simulation at 1 km resolution: establishing a performance baseline on 4888 GPUs with COSMO 5.0, *Geoscientific Model Development*, 11, 1665–1681, <https://doi.org/10.5194/gmd-11-1665-2018>, 2018.
- Gysi, T., Müller, C., Zinenko, O., Herhut, S., Davis, E., Wicky, T., Fuhrer, O., Hoefer, T., and Grosser, T.: Domain-specific multi-level IR rewriting for GPU: The Open Earth compiler for GPU-accelerated climate simulation, *ACM Transactions on Architecture and Code Optimization (TACO)*, 18, 1–23, <https://doi.org/10.1145/3469030>, 2021.
- 520 Harris, C. R., Millman, K. J., van der Walt, S. J., Gommers, R., Virtanen, P., Cournapeau, D., Wieser, E., Taylor, J., Berg, S., Smith, N. J., et al.: Array programming with NumPy, *Nature*, 585, 357–362, 2020.
- Harris, L. M. and Lin, S.-J.: A two-way nested global-regional dynamical core on the cubed-sphere grid, *Monthly Weather Review*, 141, 283–306, <https://doi.org/10.1175/mwr-d-11-00201.1>, 2013.

Hoyer, S. and Hamman, J.: xarray: ND labeled arrays and datasets in Python, *Journal of Open Research Software*, 5,   
525 <https://doi.org/10.5334/jors.148>, 2017.

Janisková, M. and Lopez, P.: Linearised physics: the heart of ECMWF’s 4D-Var, *ECMWF Newsletter No. 175*, pp. 20–26, 2023.

Janisková, M., Thépaut, J.-N., and Geleyn, J.-F.: Simplified and regular physical parameterizations for incremental four-dimensional variational assimilation, *Monthly Weather Review*, 127, 26–45, [https://doi.org/10.1175/1520-0493\(1999\)127<0026:sarppf>2.0.co;2](https://doi.org/10.1175/1520-0493(1999)127<0026:sarppf>2.0.co;2), 1999.   
530

Kim, J. Y., Kang, J.-S., and Joh, M.: GPU acceleration of MPAS microphysics WSM6 using OpenACC directives: Performance and verification, *Computers & Geosciences*, 146, 104 627, <https://doi.org/10.1016/j.cageo.2020.104627>, 2021.

Kühnlein, C., Deconinck, W., Klein, R., Malardel, S., Piotrowski, Z. P., Smolarkiewicz, P. K., Szmelter, J., and Wedi, N. P.: FVM 1.0: a nonhydrostatic finite-volume dynamical core for the IFS, *Geoscientific Model Development*, 12, 651–676,   
535 <https://doi.org/10.5194/gmd-12-651-2019>, 2019.

Kühnlein, C., Ehrenguber, T., Ubbiali, S., Krieger, N., Papritz, L., Calotiu, A., and Wernli, H.: ECMWF collaborates with Swiss partners on GPU porting of FVM dynamical core, *ECMWF Newsletter No. 175*, 175, 11–12, 2023.

Lapillonne, X., Osterried, K., and Fuhrer, O.: Using OpenACC to port large legacy climate and weather modeling code to GPUs, in: *Parallel Programming with OpenACC*, pp. 267–290, Elsevier, <https://doi.org/10.1016/b978-0-12-410397-9.00013-5>,   
540 2017.

Lapillonne, X., Sawyer, W., Marti, P., Clement, V., Dietlicher, R., Kornbluh, L., Rast, S., Schnur, R., Esch, M., Giorgetta, M., et al.: Global climate simulations at 2.8 km on GPU with the ICON model, in: *EGU General Assembly Conference Abstracts*, p. 10306, <https://doi.org/10.5194/egusphere-egu2020-10306>, 2020.

Lawrence, B. N., Rezny, M., Budich, R., Bauer, P., Behrens, J., Carter, M., Deconinck, W., Ford, R., Maynard, C., Mullerworth,   
545 S., et al.: Crossing the chasm: how to develop weather and climate models for next generation computers?, *Geoscientific Model Development*, 11, 1799–1821, <https://doi.org/10.5194/gmd-11-1799-2018>, 2018.

Lindfield, G. and Penny, J.: *Numerical Methods: Using MATLAB*, Academic Press, 2018.

Luz, M., Gopal, A., Ong, C. R., Müller, C., Hupp, D., Burgdorfer, N., Farabullini, N., Bösch, F., Dipankar, A., Bianco, M., et al.: A GT4Py-Based Multi-Node Standalone Python Implementation of the ICON Dynamical Core, *Platform for   
550 Advanced Scientific Computing (PASC) Conference*, Zurich, Switzerland, 3–5 June, 2024, 2024.

McGibbon, J., Brenowitz, N. D., Cheeseman, M., Clark, S. K., Dahm, J. P., Davis, E. C., Elbert, O. D., George, R. C., Harris, L. M., Henn, B., et al.: fv3gfs-wrapper: a Python wrapper of the FV3GFS atmospheric model, *Geoscientific Model Development*, 14, 4401–4409, <https://doi.org/10.5194/gmd-14-4401-2021>, 2021.

- Melvin, T., Benacchio, T., Shipway, B., Wood, N., Thuburn, J., and Cotter, C.: A mixed finite-element, finite-volume, semi-implicit discretization for atmospheric dynamics: Cartesian geometry, *Quarterly Journal of the Royal Meteorological Society*, 145, 2835–2853, 2019.
- Melvin, T., Shipway, B., Wood, N., Benacchio, T., Bendall, T., Boutle, I., Brown, A., Johnson, C., Kent, J., Pring, S., et al.: A mixed finite-element, finite-volume, semi-implicit discretisation for atmospheric dynamics: Spherical geometry, *Quarterly Journal of the Royal Meteorological Society*, 2024.
- Méndez, M., Tinetti, F. G., and Overbey, J. L.: Climate models: challenges for Fortran development tools, in: 2014 Second International Workshop on Software Engineering for High Performance Computing in Computational Science and Engineering, pp. 6–12, IEEE, <https://doi.org/10.1109/se-hpccse.2014.7>, 2014.
- Monteiro, J. M., McGibbon, J., and Caballero, R.: sympl (v. 0.4.0) and climt (v. 0.15.3) – Towards a flexible framework for building model hierarchies in Python, *Geoscientific Model Development*, 11, 3781–3794, <https://doi.org/10.5194/gmd-11-3781-2018>, 2018.
- Müller, A., Deconinck, W., Kühnlein, C., Mengaldo, G., Lange, M., Wedi, N., Bauer, P., Smolarkiewicz, P. K., Diamantakis, M., Lock, S.-J., et al.: The ESCAPE project: energy-efficient scalable algorithms for weather prediction at exascale, *Geoscientific Model Development*, 12, 4425–4441, <https://doi.org/10.5194/gmd-12-4425-2019>, 2019.
- Neumann, P., Düben, P., Adamidis, P., Bauer, P., Brück, M., Kornblüeh, L., Klocke, D., Stevens, B., Wedi, N., and Biercamp, J.: Assessing the scales in numerical weather and climate predictions: will exascale be the rescue?, *Philosophical Transactions of the Royal Society A*, 377, 20180148, <https://doi.org/10.1098/rsta.2018.0148>, 2019.
- Nishino, R. and Loomis, S. H. C.: CuPy: A NumPy-compatible library for NVIDIA GPU calculations, 31st conference on neural information processing systems, p. 151, 2017.
- Nogherotto, R., Tompkins, A. M., Giuliani, G., Coppola, E., and Giorgi, F.: Numerical framework and performance of the new multiple-phase cloud microphysics scheme in RegCM4.5: precipitation, cloud microphysics, and cloud radiative effects, *Geoscientific Model Development*, 9, 2533–2547, <https://doi.org/10.5194/gmd-9-2533-2016>, 2016.
- Randall, D. A., Hurrell, J. W., Gettelman, A., Loft, R., Skamarock, W. C., Hauser, T., Dazlich, D. A., and Sun, L.: Simulations With EarthWorks, in: AGU Fall Meeting Abstracts, vol. 2022, pp. A33E–02, 2022.
- Schär, C., Fuhrer, O., Arteaga, A., Ban, N., Charpilloz, C., Di Girolamo, S., Hentgen, L., Hoefler, T., Lapillonne, X., Leutwyler, D., et al.: Kilometer-scale climate models: Prospects and challenges, *Bulletin of the American Meteorological Society*, <https://doi.org/10.1175/bams-d-18-0167.1>, 2019.
- Schulthess, T. C., Bauer, P., Wedi, N., Fuhrer, O., Hoefler, T., and Schär, C.: Reflecting on the goal and baseline for exascale computing: A roadmap based on weather and climate simulations, *Computing in Science & Engineering*, 21, 30–41, <https://doi.org/10.1109/mcse.2018.2888788>, 2018.

- 585 Shipman, G. M. and Randles, T. C.: An evaluation of risks associated with relying on Fortran for mission critical codes for the next 15 years, <https://doi.org/10.2172/1970284>, 2023.
- Smolarkiewicz, P. K., Deconinck, W., Hamrud, M., Kühnlein, C., Mozdzynski, G., Szmelter, J., and Wedi, N. P.: A finite-volume module for simulating global all-scale atmospheric flows, *Journal of Computational Physics*, 314, 287–304, <https://doi.org/10.1016/j.jcp.2016.03.015>, 2016.
- 590 Taylor, M. A., Guba, O., Steyer, A., Ullrich, P. A., Hall, D. M., and Eldred, C.: An energy consistent discretization of the nonhydrostatic equations in primitive variables, *Journal of Advances in Modeling Earth Systems*, 12, e2019MS001783, <https://doi.org/10.1029/2019ms001783>, 2020.
- Ubbiali, S., Schär, C., Schlemmer, L., and Schulthess, T. C.: A numerical analysis of six physics-dynamics coupling schemes for atmospheric models, *Journal of Advances in Modeling Earth Systems*, 13, e2020MS002377, <https://doi.org/10.1029/2020ms002377>, 2021.
- 595 Ubbiali, S., Kühnlein, C., Schär, C., Schlemmer, L., Schulthess, T. C., Staneker, M., and Wernli, H.: Data and scripts for the manuscript “Exploring a high-level programming model for the NWP domain using ECMWF microphysics schemes” (v0.1.0), Zenodo, <https://doi.org/10.5281/zenodo.11155353>, 2024a.
- Ubbiali, S., Kühnlein, C., Schär, C., Schlemmer, L., Schulthess, T. C., and Wernli, H.: ifs-physics-common: v0.1.0, Zenodo, <https://doi.org/10.5281/zenodo.11153742>, 2024b.
- 600 Ubbiali, S., Kühnlein, C., and Wernli, H.: gt4py-dwarf-p-cloudsc: v0.1.0, Zenodo, <https://doi.org/10.5281/zenodo.11155001>, 2024c.
- Ubbiali, S., Kühnlein, C., and Wernli, H.: gt4py-dwarf-p-cloudsc2-tl-ad: v0.1.0, Zenodo, <https://doi.org/10.5281/zenodo.11155036>, 2024d.
- 605 Watkins, J., Carlson, M., Shan, K., Tezaur, I., Perego, M., Bertagna, L., Kao, C., Hoffman, M. J., and Price, S. F.: Performance portable ice-sheet modeling with MALI, *The International Journal of High Performance Computing Applications*, 37, 600–625, <https://doi.org/10.1177/10943420231183688>, 2023.
- Yang, Z., Halem, M., Loft, R., and Suresh, S.: Accelerating MPAS-A model radiation schemes on GPUs using OpenACC, in: *AGU Fall Meeting Abstracts*, vol. 2019, pp. A11A–06, 2019.
- 610 Zängl, G., Reinert, D., Rípodas, P., and Baldauf, M.: The ICON (ICOsahedral Non-hydrostatic) modelling framework of DWD and MPI-M: Description of the non-hydrostatic dynamical core, *Quarterly Journal of the Royal Meteorological Society*, 141, 563–579, <https://doi.org/10.1002/qj.2378>, 2015.